Harmonic Instability Source Identification in Large Wind Farms

Ebrahimzadeh, Esmaeil; Blaabjerg, Frede; Wang, Xiongfei; Bak, Claus Leth

Published in:
Proceedings of 2017 IEEE Power & Energy Society General Meeting

DOI (link to publication from Publisher):
10.1109/PESGM.2017.8274020

Publication date:
2017

Document Version
Accepted author manuscript, peer reviewed version

Harmonic Instability Source Identification in Large Wind Farms

Esmaeil Ebrahimzadeh, Frede Blaabjerg, Xiongfei Wang, and Claus Leth Bak

Department of Energy Technology
Aalborg University
Aalborg, Denmark
ebb@et.aau.dk, fbl@et.aau.dk, xwa@et.aau.dk, and clb@et.aau.dk

***Abstract*— A large-scale power electronics based power system like a wind farm introduces the passive and active impedances. The interactions between the active and passive impedances can lead to harmonic-frequency oscillations above the fundamental frequency, which can be called harmonic instability. This paper presents an approach to identify which wind turbine and which bus has more contribution to the harmonic instability problems. In the approach, a wind farm is modeled as a Multi-Input Multi-Output (MIMO) dynamic system. The poles of the MIMO transfer matrix are used to predict the system instability and the eigenvalues sensitivity analysis in respect to the elements of the MIMO matrix locates the most influencing buses of the wind farm. Time-domain simulations in PSCAD software environment for a 400-MW wind farm validate that the presented approach is an effective tool to determine the main source of the instability problems.**

Keywords—harmonics; power quality; wind farm; stability; multi-input mulit-output dynamic system

I. INTRODUCTION

High penetration of power electronic converters into the electric power system has initiated technical challenges in respect to the stability and power quality of the system [1]. In a large power electronics based power system like a wind farm, the cables, transformers, capacitor banks, shunt reactors, etc., present the passive impedances, while power electronic converters present the active impedances [2]. The mutual interactions between the passive and active impedances may lead to instability problems [3]. The interactions of the active impedances resulting from the fast inner control loops of the power converters may lead to high frequency oscillations above the fundamental frequency, which can be called harmonic instability [4]. Many of researches about harmonic instability discuss how to predict the instability conditions but pay less much attention to identify the main source of instability [4]- [14]. For stability analysis, a general approach is based on the state-space model, where the contribution of each component to the system stability can be identified by the participation factor analysis [4]-[9]. However, since the detailed models of power converters, loads, cables, transformers, etc, are required, the formulation of the state matrices for systems with a high integration of power converters may become complicated [10]. Apart from the state-space analysis, the impedance-based analysis approach is effective tool to predict the harmonic instability by calculating the ratio of the converter active impedance to the grid equivalent impedance at Point of Common Coupling (PCC) [11]-[14]. However, it cannot identify which bus and which converter in a large power electronics based power systems contribute more to the harmonic instability.

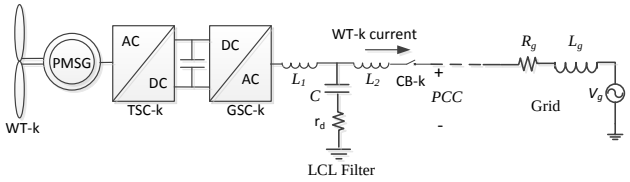

(a)

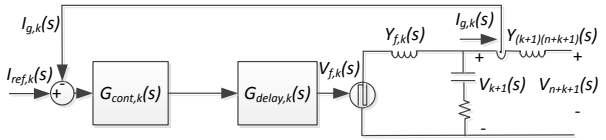

(b)

Fig. 1. Wind Turbine (WT) with (a) full-scale power converters with LCL filter, (b) the control diagram the k^{th} Grid-Side Converter (GSC) of the WT for harmonic stability analysis.

Another powerful tool for predicting instability problems is presented in [15], [16], where a wind farm is introduced as a Multi-Input Multi-Output (MIMO) dynamic system by using a transfer function matrix including passive elements and converter controller parameters. However, the contributions of different components and buses on harmonic-frequency oscillations have not been identified.

In order to fill in this gap, this paper presents an analytical approach to calculate participation factors of the different buses and converters in a wind farm. The participation factors of the different components and buses are calculated by means of modal analysis of the introduced MIMO system. A power converter with a larger participation factor has more contribution to the harmonic instability, and consequently, a power converter with the largest participation factor is identified as the main source of harmonic instability. The proposed methodology has been verified by time-domain simulations of a 400-MW wind farm in PSCAD software environment.

II. A LARGE WIND FARM AS A MULTI-INPUT MULTI-OUTPUT DYNAMIC SYSTEM

Fig. 1(a) shows an Wind Turbine (WT) with full-scale converters in a wind farm and Fig. 1(b) depicts the equivalent circuit of the Grid-Side Converter (GSC) of the WT for harmonic stability analysis. In Fig. 1(b), $G_{cont,k}$ is the current controller, and $G_{delay,k}$ is the approximated delay of the digital control. In this paper, $G_{cont,k}$ and $G_{delay,k}$ are assumed to be as

$$G_{cont,k} = K_{p,k} + \frac{K_{i,k}s}{s^2 + \omega_f^2} \tag{1}$$

$$G_{delay,k} = e^{-1.5T_{s,k}s} \approx \frac{1 - \frac{1.5T_{s,k}}{2}s + \frac{(1.5T_{s,k})^2}{10}s^2 - \frac{(1.5T_{s,k})^3}{120}s^3}{1 + \frac{1.5T_{s,k}}{2}s + \frac{(1.5T_{s,k})^2}{10}s^2 + \frac{(1.5T_{s,k})^3}{120}s^3} \tag{2}$$

where ω_f is the fundamental frequency of the grid and $T_{s,k}$ is the sampling period. The objective of this paper is to identify the main source of harmonic instability (harmonic-frequency oscillations above the fundamental frequency). Therefore, outer power control and dc-link oscillations, which may cause low frequency oscillations, are neglected [11]. Since the dc-link is considered constant, the Turbine-Side Converters (TSCs) can also be neglected. The relationship between the current references and the bus voltages in the wind farm can be written as a Multi-Input Multi-Output (MIMO) dynamic system by

$$\mathbf{V(s) = G_f^{-1}(s)U(s)} \tag{3}$$

V(s), $\mathbf{G_f(s)}$, and **U(s)** are

$$\mathbf{V(s)} = \begin{bmatrix} \mathbf{V_o(s)} \\ \mathbf{V_z(s)} \end{bmatrix} \mathbf{G_f(s)} = \begin{bmatrix} \mathbf{G_1(s)} & \mathbf{G_2(s)} \\ \mathbf{G_3(s)} & \mathbf{G_4(s)} \end{bmatrix} \mathbf{U(s)} = \begin{bmatrix} \mathbf{U_{ref}(s)} \\ \mathbf{U_z(s)} \end{bmatrix} \tag{4}$$

where

$$\mathbf{U_{ref}(s)} = \begin{bmatrix} V_g(s) \\ I_{ref,1}(s) \\ I_{ref,2}(s) \\ \vdots \\ I_{ref,n}(s) \end{bmatrix} \mathbf{V_o(s)} = \begin{bmatrix} V_1(s) \\ V_2(s) \\ V_3(s) \\ \vdots \\ V_{n+1}(s) \end{bmatrix}$$
$$\mathbf{V_z(s)} = \begin{bmatrix} V_{n+2}(s) \\ \vdots \\ V_{n+m}(s) \end{bmatrix} \mathbf{U_z(s)} = \begin{bmatrix} 0 \\ \vdots \\ 0 \end{bmatrix} \tag{5}$$

$\mathbf{G_1(s)}$, $\mathbf{G_2(s)}$, $\mathbf{G_3(s)}$, and $\mathbf{G_4(s)}$ are given in [16]. $V_i(s)$ is the voltage of i^{th} bus, $I_{ref,k}(s)$ is the current reference of the k^{th} GSC, and the $V_g(s)$ is the main grid voltage.

A. Poles of the system

Poles of the MIMO dynamic system can be obtained by solving the following equation:

$$\begin{aligned} &\det\left[\mathbf{G_f(s)}\right] = 0 \\ &\Rightarrow P_1 = \alpha_1 + \mathrm{j}\beta_1, P_2 = \alpha_2 + \mathrm{j}\beta_2, \cdots, P_q = \alpha_q + \mathrm{j}\beta_q \end{aligned} \tag{6}$$

where the oscillation frequency (f_i) and the damping ratio (ζ_i) of oscillations can also be obtained as

$$f_i = \frac{\beta_i}{2\pi} \qquad \zeta_i = \frac{-\alpha_i}{\sqrt{\alpha_i^2 + \beta_i^2}} \tag{7}$$

The system is stable if and only if the all poles have negative real parts. The pole with the largest real part is called the critical pole (s_c), i.e.,

$$s_c = \alpha_c + j\beta_c \quad \alpha_c = Max(\alpha_1, \alpha_2, \cdots, \alpha_q) \tag{8}$$

B. Harmonic Instability source identification

By substituting the critical pole (s_c) for s in the function matrix of $\mathbf{G_f(s)}$, $\mathbf{G_f(s_c)}$ can be numerically obtained. Based on the idea of the eigenvalue decomposition [17]-[21], the matrix $\mathbf{G_f(s_c)}$ can be decomposed into three matrixes as

$$\mathbf{G_f(s_c) = R_f \Lambda_f L_f} = \mathbf{R_f} \begin{bmatrix} \lambda_1 & 0 & 0 & 0 \\ 0 & \lambda_2 & 0 & 0 \\ 0 & 0 & \cdots & 0 \\ 0 & 0 & 0 & \lambda_m \end{bmatrix} \mathbf{L_f} \tag{9}$$

where $\mathbf{\Lambda_f}$ is a diagonal matrix whose diagonal elements are the eigenvalues of $\mathbf{G_f(s_c)}$ ($\lambda_1, \lambda_2, \ldots, \lambda_m$). $\mathbf{R_f}$ is a matrix whose columns are the corresponding right eigenvectors, i.e.,

$$\mathbf{G_f(s_c)R_f = R_f \Lambda_f} \tag{10}$$

$\mathbf{L_f}$ is a matrix whose rows are transposed left eigenvectors, i.e,

$$\mathbf{L_f G_f(s_c) = \Lambda_f L_f} \tag{11}$$

The following equation can be derived from (10) and (11):

$$\mathbf{L_f = R_f^{-1}} \tag{12}$$

Using (9) and (12), the inverse of $\mathbf{G_f(s_c)}$ can be calculated from

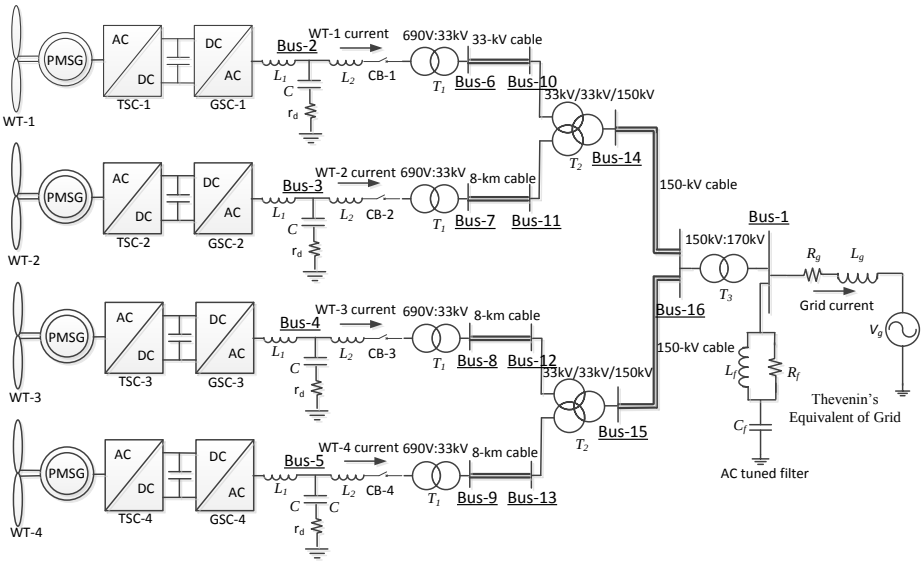

Fig. 2. The configuration of the 400-MW wind farm with the aggregated strings which is studied in this paper.

Table I. Frequency, damping, the largest participation factor, and the most influencing bus for the oscillatory modes of the wind farm

Pole i	Real part α_i	Frequency f_i	Damping ζ_i	The largest Participation Factor (PF_i)	The most influencing bus
1	-107.438	51.40616	0.315628	0.535925	Bus-2
2	-65.7248	52.29672	0.196136	0.36575	Bus-3
3	-76.9366	56.52478	0.211717	0.185176	Bus-4
4	-361	62.88671	0.674504	0.234466	Bus-5
6	-884.23	508.8612	0.266552	1.233141	Bus-2
7	-558.831	834.3687	0.105996	0.598959	Bus-2
8	62.19831	840.1478	-0.01178	0.431535	Bus-2
9	-36.3585	889.9904	0.006502	0.253933	Bus-2
10	-778.346	900.1397	0.136335	0.791803	Bus-5
11	-1466.69	908.4157	0.24888	0.633163	Bus-2
12	-966.408	1010.935	0.150414	0.963276	Bus-4
13	-146.546	1262.467	0.018471	0.259429	Bus-16
15	-13453.3	1520.601	0.815316	0.989698	Bus-2
17	-13060.2	1571.691	0.797646	0.990838	Bus-3
18	-12976.1	1595.823	0.791289	0.993135	Bus-5
20	-12659.8	1664.792	0.770898	0.996	Bus-4
21	-172.072	2396.805	0.011425	0.288203	Bus-8
22	-193.822	2400.508	0.012849	0.28709	Bus-7
23	-90.7824	2646.583	0.005459	0.273503	Bus-9
24	-95.4275	2649.73	0.005732	0.272747	Bus-6
25	-57.638	6464.016	0.001419	0.288726	Bus-10
26	-57.9728	6464.04	0.001427	0.288816	Bus-13
27	-56.9193	6480.975	0.001398	0.291282	Bus-11

Table II. Participation factors of the buses 2 to 5 for the critical pole

Bus number	PF for the critical pole (P_8=62.2±5279i)
Bus-2 (GSC-1)	0.43
Bus-3 (GSC-2)	0.09
Bus-4 (GSC-3)	0.16
Bus-5 (GSC-4)	0.14

$$\mathbf{G_f^{-1}(s_c) = R_f \Lambda_f^{-1} L_f = R_f} \begin{bmatrix} 1/\lambda_1 & 0 & 0 & 0 \\ 0 & 1/\lambda_2 & 0 & 0 \\ 0 & 0 & \cdots & 0 \\ 0 & 0 & 0 & 1/\lambda_m \end{bmatrix} \mathbf{L_f} \quad (13)$$

Since s_c is a pole of the $\mathbf{G_f^{-1}(s)}$, one of the eigenvalues of $\mathbf{G_f(s_c)}$ (λ_1, λ_2, ..., or λ_m) should ideally be equal to zero. However, it is close to, but not exactly zero, because the decomposition is performed using floating-point computations, which can suffer from round-off errors. The mentioned eigenvalue, i.e, the smallest eigenvalue is called the critical eigenvalue (λ_c) and its right and left eigenvectors are called the critical right and left eigenvectors ($\mathbf{r_c}$ and $\mathbf{l_c}$). If the i^{th} eigenvalue is λ_c, the i^{th} column of the matrix $\mathbf{R_f}$ is $\mathbf{r_c}$ and the i^{th} row of the matrix $\mathbf{L_f}$ is $\mathbf{l_c}$. The sensitivity of the critical eigenvalue with respect to the $\mathbf{G_f(s_c)}$ entries can then be obtained by

$$\mathbf{S_{\lambda c} = r_c l_c} \quad (14)$$

$\mathbf{S_{\lambda c}}$ is the sensitivity matrix and its k^{th} diagonal element is Participation Factor (PF) of the k^{th} bus. The bus with the largest PF is the most influencing bus on the critical eigenvalue, where, in fact, is the main source of the instability and can be called the critical bus.

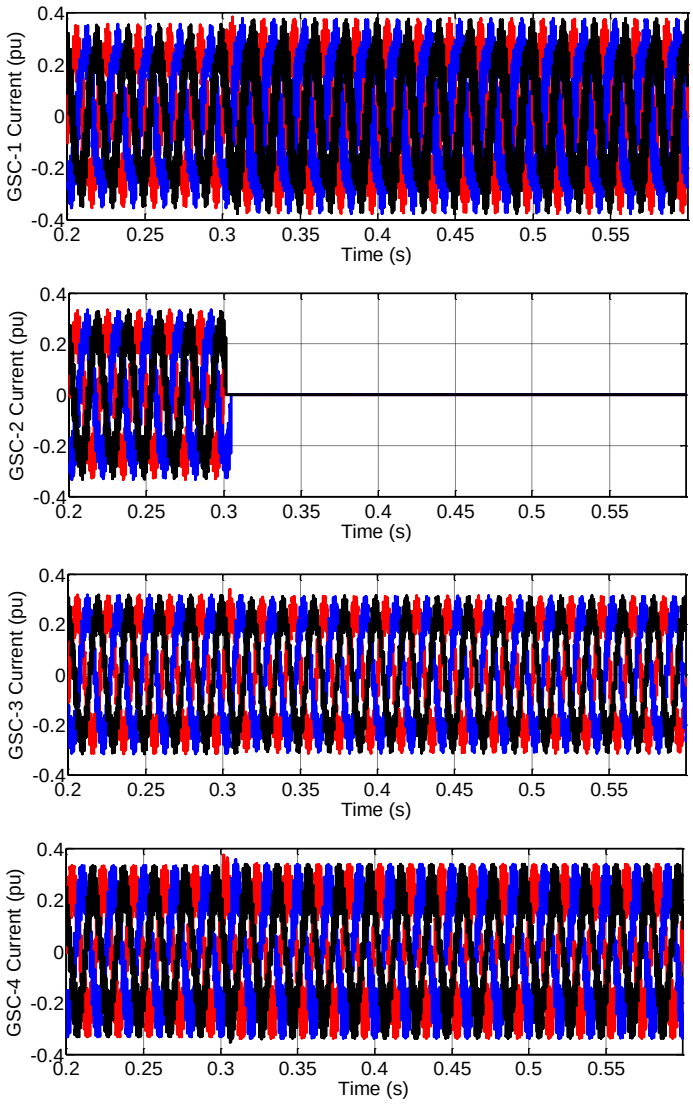

Fig. 3. Disconnecting the power converter (GSC-2) with the small Participation Factor (PF) under unstable conditions at t = 0.3 s.

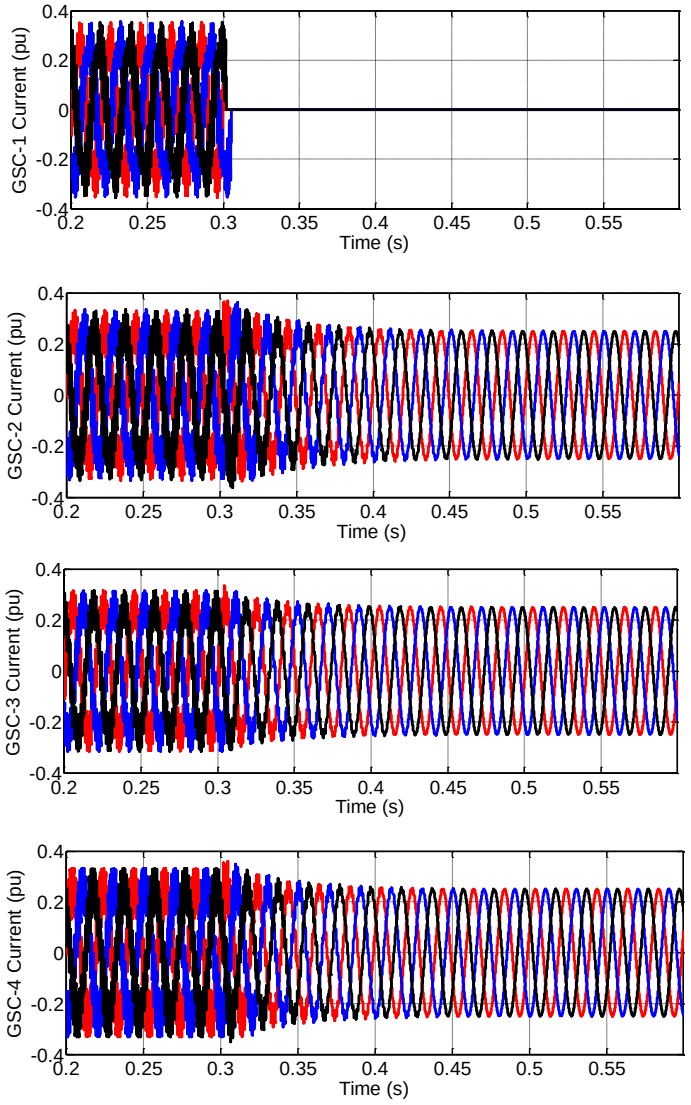

Fig. 4. Disconnecting the power converter (GSC-1) with the large Participation Factor (PF) under unstable conditions at t = 0.3 s.

III. A 400-MW WIND FARM AS A CASE STUDY

A. *Theoretical analysis*

Fig. 2 shows the configuration of a 400-MW wind farm [10], which is used in this paper to identify the harmonic instability source. The network consists of four branches and each branch is an aggregated 100-MW wind turbine. A simple Thévenin's equivalent voltage source is used to represent the grid. The transformers are modeled as a short-circuit impedance and the cables are modeled as a nominal π-model. In this case study, the dimension of the matrix $\mathbf{G_f(s_c)}$ is 16×16, which shows the relations between Bus-1 to Bus-16 (see Fig. 2). The parameters of the wind farm are given in Appendix A. The GSC controllers are designed with acceptable bandwidths. More detailed information about the model can be found in [16], [22], [23]. Table I shows the oscillation frequency, the damping ratio, the largest participation factor, and the most influencing bus for the oscillatory modes of the wind farm. It can be seen that most poles with low and medium frequencies are related to power electronic converter (Bus-2 to Bus-5) and high-frequency poles are related to the buses where power cables and transformers are connected. The wind farm has one unstable pole, P_8, (critical pole) with the frequency of 840 Hz. Therefore, harmonic-frequency oscillations around 840 Hz propagate into the wind farm because of instability problems. Bus-2 has the largest PF for the critical pole, which shows that the GCS-1 is the main source of the harmonic instability. Table II shows the participation factors of the buses 2 to 5 for the critical pole. As it can be seen from Table II, Bus-2 (GSC-1) is the most influencing bus on instability, while Bus-3 (GSC-2) is less critical compared to the other buses.

B. Time-domain simulation results

In order to confirm the predicted theoretical results, time-domain simulations have been provided in the PSCAD software environment. In Fig. 3, the GSC-2 is disconnected from the wind farm at t = 0.3s. Since the GCS-2 (Bus-3) has a very small PF (PF = 0.09), the wind farm will be remained unstable even after disconnecting the GSC-2. In Fig. 4, the GSC-1, the converter with the largest PF (PF = 0.43) is disconnected. Fig. 4 shows the wind farm becomes stable after disconnecting the GSC-1, which confirms the GSC-1 is the main source of the instability (as predicted in Table II).

IV. CONCLUSION

This paper has attempted to identify the contribution of each power converter to harmonic instability and to locate the main source of harmonic instability in large wind farms. A large wind farm is introduced as a Multi-Input Multi-Output (MIMO) dynamic system and the critical converter are identified by the modal analysis of the introduced MIMO system. Under unstable conditions, the theoretical analysis for a 400-MW wind farm shows that some power converters can have larger Participation Factor (PF) than the other converters. Time-domain simulations in PSCAD software confirm that disconnecting the power converters with larger PFs can transform the wind farm from an unstable condition to a stable condition.

V. APPENDIX A

TABLE A. 400-MW WIND FARM PARAMETERS

Parameter		Value (P.U.)
Transformer T_1	***Leakage inductance***	3.18×10^{-4}
33 kV cable (Cable $_{33\text{-kv}}$)	***Shunt capacitance***	7.841×10^{-6}
	Series inductance	1.802×10^{-4}
	Series resistance	0.022
Transformer T_2	***Leakage inductance***	3.8×10^{-4}
150 kV cable (Cable $_{150\text{-kv}}$)	***Shunt capacitance***	7.54×10^{-5}
	Series inductance	5.8×10^{-4}
	Series resistance	0.018
Transformer T_3	***Leakage inductance***	4.46×10^{-4}
AC tuned filter	***Resistance (R_f)***	2
	Inductance (L_f)	10.612×10^{-6}
	Capacitance (C_f)	9.55×10^{-5}
Grid	***X/R ratio***	10
	SCR	5
Controller Bandwith	***GSC-1***	710 Hz
	GSC-2	450 Hz
	GSC-3	625 Hz
	GSC-4	780 Hz

S_{base} = 450 MVA, f_b = 50 Hz

REFERENCES

[1] Z. Chen, J. M. Guerrero, and F. Blaabjerg, "A review of the state of the art of power electronics for wind turbines," *IEEE Trans. Power Electron.*, vol. 24, no. 8, pp. 1859-1875, Aug. 2009.

[2] M. Cespedes and J. Sun, "Impedance modeling and analysis of grid connected voltage-source converters," *IEEE Trans. Power Electron.*, vol. 29, no. 3, pp. 1254–1261, Mar. 2014.

[3] L. H. Kocewiak, J. Hjerrild, and C. L. Bak, "Wind turbine converter control interaction with complex wind farm systems," *IET Renewable Power Generation*, vol. 7, no. 4, pp. 380–389, Jul. 2013.

[4] N. Pogaku, M. Prodanovic, and T. C. Green, "Modeling, analysis and testing of autonomous operation of an inverter-based microgrid," *IEEE Trans. Power Electron*., vol. 22, no. 2, pp. 613–625, Mar. 2007.

[5] N. Bottrell, M. Prodanovic, and T. C. Green, "Dynamic stability of a microgrid with an active load," *IEEE Trans. Power Electron.*, vol. 28, no.11, pp. 5107-5119, Nov. 2013.

[6] A. Singh, and A. K. Kaviani, and B. Mirafzal, "On dynamic models and stability analysis of three-phase phasor PWM-Based CSI for stand-alone applications," *IEEE Trans. Ind. Electron*., vol. 62, no. 5, pp. 2698-2707, May. 2015.

[7] E. A. A. Coelho, P. C. Cortizo, and P. F. D. Garcia, "Small-signal stability for parallel-connected inverters in stand-alone AC supply systems," *IEEE Trans. Ind. App.*, vol. 38, no. 2, pp. 533-542, Mar. 2002.

[8] L. P. Kunjumuhammed, B. C. Pal, C. Oates and K. J. Dyke, "Electrical oscillations in wind farm systems: analysis and insight based on detailed modeling," *Trans. Sustain. Energy*, vol. 7, no. 1, pp. 51-62, Jan. 2016.

[9] L. P. Kunjumuhammed; B. C. Pal; C. Oates; K. Dyke, "The Adequacy of the present practice in dynamic aggregated modelling of Wind Farm Systems," *Trans. Sustain. Energy*, vol.PP, no.99, pp.1-1

[10] X. Wang, F. Blaabjerg, and W. Wu, "Modelling and analysis of harmonic stability in ac power-electronics-based power system," *IEEE Trans. Power Electron*. , vol. 29, no. 12, pp.6421 -6432, Dec. 2014.

[11] J. Sun, "Impedance-based stability criterion for grid-connected inverters," *IEEE Trans. Power Electron.*, vol. 26, no. 11, pp. 3075–3078, Nov. 2011.

[12] L. Xu and L. Fan, "Impedance-based resonance analysis in a VSC-HVDC system," *IEEE Trans. Power Del*., vol. 28, no. 4, pp. 2209–2216, Oct. 2013.

[13] L. Xu, L. Fan and Z. Miao, "DC impedance-model-based resonance analysis of a VSC–HVDC system," *IEEE Trans. Power Del*, vol. 30, no. 3, pp. 1221-1230, June 2015.

[14] C. Yoon, H. Bai, R. Beres, X. Wang, C. Bak, and F. Blaabjerg, "Harmonic stability assessment for multi-paralleled, grid-connected inverters," accepted for publication in *Trans. Sustain. Energy*: doi: 10.1109/TSTE.2016.2551737

[15] E. Ebrahimzadeh, F. Blaabjerg, X. Wang, C. Leth Bak, "Modeling and identification of harmonic instability problems in wind farms," in *Proc. of IEEE ECCE*, USA, Sep. 2016, pp. 1-6.

[16] E. Ebrahimzadeh, F. Blaabjerg, X. Wang, C. Leth Bak, "Efficient approach for harmonic resonance identification of large wind power plants," in *Proc. of IEEE PEDG*, Canada, Jun. 2016, pp. 1-7.

[17] S. Skogestad and I. Postlethwaite, Multivariable feedback control: analysis and design, New York: Wiley, 2000.

[18] P. Kundur, Power system stability and control. New York: McGraw-Hill, 1994.

[19] W. Xu, Z. Huang, Y. Cui, and H. Wang, "Harmonic resonance mode analysis," *IEEE Trans. Power Del*., vol. 20, no. 2, pp. 1182-1190, Apr. 2005.

[20] Y. Cui and X. Wang, "Modal frequency sensitivity for power system harmonic resonance analysis," *IEEE Trans. Power Del.*, vol. 27, no. 2, pp. 1010–1017, Apr. 2012.

[21] K. N. B. M. Hasan, K. Rauma, A. Luna, J. I. Candela, and P. Rodriguez,"Harmonic compensation analysis in offshore wind power plants using hybrid filters," *IEEE Trans. Ind. Appl.*, vol. 50, no. 3, pp. 2050–2060, May/Jun. 2014.

[22] E. Ebrahimzadeh, F. Blaabjerg, X. Wang, C. Leth Bak, "Efficient approach for harmonic resonance identification of large wind power plants," in *Proc. of IEEE PEDG*, Canada, Jun. 2016, pp. 1-7.

[23] S. K. Chaudhary, "Control and protection of wind power plants with VSC-HVDC connection," (PhD Thesis, Aalborg University, Aalborg, Denmark, 2011.